

# Characteristic Changes of Bond Energies for Gas-Phase Cluster Ions of Halide Ions with Methane and Chloromethanes

Kenzo Hiraoka,\* Takayuki Mizuno, Tomoyuki Iino, and Daisuke Eguchi

Faculty of Engineering, Yamanashi University, Takeda-4, Kofu 400-8511, Japan

Shinichi Yamabe\*

Department of Chemistry, Nara University of Education, Takabatake-cho, Nara 630-8528, Japan

Received: January 10, 2001; In Final Form: March 8, 2001

Gas-phase equilibria for clustering reactions of both halide ions ( $X^-$ ) with methane and chloride ions with chloromethanes ( $CH_{4-m}Cl_m$ ) were measured with a pulsed electron-beam high-pressure mass spectrometer. The bond energies were found to show irregular decreases for  $F^-(CH_4)_n$ , with  $n = 6$  and  $8$ , for  $Cl^-(CH_3Cl)_n$ , with  $n = 2, 4$ , and  $6$ , and for  $Cl^-(CH_2Cl_2)_n$ , with  $n = 2$  and  $4$ . These even numbers indicate that the core ions are preferably solvated by the ligands with these  $n$  values. The theoretical calculation revealed that the cluster ion  $Cl^-(CCl_4)$  has the structure of  $[Cl...ClCCl_3]^-$  rather than  $Cl^-...Cl_3CCl$ . The unexpectedly large bond energy for  $Cl^-(CCl_4)$  (13.4 kcal/mol) is due to the charge dispersal in the complex  $[Cl...ClCCl_3]^-$ .

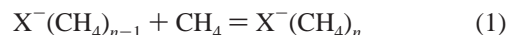
## 1. Introduction

Charge-transfer salts of organic donor molecules with mono-negative ions can be insulating, semiconducting, or metallic at room temperature.<sup>1</sup> When the temperature is lowered, some salts become superconducting as well. The bond energies for the cluster ions of halide ions  $X^-$  with organic molecules would give the fundamental information on the properties of the charge-transfer complexes. However, the bond energies of  $X^-$  with the hydrocarbon have not been measured so far despite the fundamental combination. Novoa et al. carried out SCF and MP2 calculations on the bond energies and structures of  $X^-(CH_4)$ .<sup>2</sup> They predicted that the most stable structures for complexes  $X^-(CH_4)$  have the  $C_{3v}$  geometries of the type  $X^-...H-C\equiv H_3$ . In the present study, the thermodynamic stabilities of the cluster ions  $X^-(CH_4)_n$  were measured down to the low temperature limit. The nature of bonding is found to be mainly electrostatic. The cluster ion  $F^-(CH_4)_n$  was found to have the shell structure with  $n = 6$  and  $8$ .

The gas-phase  $S_N2$  reactions have been investigated experimentally and theoretically<sup>3–14</sup> because this reaction is of paramount importance in organic chemistry. The study of the binding of gas-phase halide ions to Brønsted acids gives the fundamental information on the  $S_N2$  reactions.<sup>15</sup> In this study, the thermochemical stabilities and structures of the cluster ions of  $Cl^-$  with chloromethanes ( $CH_{4-m}Cl_m$ ) were investigated. The irregular decrease of the bond energies was observed for  $Cl^-(CH_3Cl)_n$ , with  $n=2, 4$ , and  $6$ , and for  $Cl^-(CH_2Cl_2)_n$ , with  $n = 2$  and  $4$ . The unexpectedly large bond energy (13.4 kcal/mol) measured for  $Cl^-(CCl_4)_1$  is found to be due to the charge dispersal in the complex  $[Cl...Cl...CCl_3]^-$ . This bonding pattern is unique because the original mechanism proposed by Brauman and co-workers for the nucleophilic substitution reaction,  $Cl^- + CH_3Cl = ClCH_3 + Cl^-$ , is an indirect backside attack in which a  $Cl^-...H_3CCl$  ion-dipole complex is formed prior to surmounting the central barrier and forming product.<sup>3</sup> A surprising result that “the  $Cl^- \rightarrow ClCCl_3$  head-on model” gives the large bond energy will be discussed.

## 2. Experimental and Theoretical Methods

The experiments were made with a pulsed electron beam high-pressure mass spectrometer.<sup>16,17</sup> Equilibrium measurements for the clustering reaction 1 ( $X^-$ , halide ion) were made by introducing  $X^-$ -forming reagent gases ( $NF_3$  for  $F^-$ ,  $CCl_4$  for  $Cl^-$ ,  $CH_2Br_2$  for  $Br^-$ , and  $CH_3I$  for  $I^-$ ) into the  $\sim 3$  Torr reagent  $CH_4$  gas through a stainless steel capillary.



For the clustering reaction 2



small amounts of  $Cl^-$ -forming reagent gas  $CCl_4$  and reagent gases  $CH_{4-m}Cl_m$  (i.e.,  $CH_3Cl$ ,  $CH_2Cl_2$ ,  $CHCl_3$ ) were introduced through stainless steel capillaries.

The measurements were made down to the low-temperature limit at which reagent gases started to condense on the wall of the ion source.

To assess the experimental bond energies, we performed density-functional-theory and ab initio calculations. Geometries of  $X^-(CH_4)_n$  and  $Cl^-(CH_{4-m}Cl_m)_n$  ( $n = 1-4$ ) were optimized using the B3LYP/6-31+G\* method.<sup>18</sup> The diffuse function (+) is indispensable to describing properly anionic systems.<sup>19</sup> Subsequent vibrational analyses were made to check whether the obtained geometries are correctly at the energy minima and to obtain the zero-point vibrational energies (ZPEs). To evaluate electronic energies of  $n = 0$  and  $1$  accurately, we made single-point calculations at QCISD(T)/6-311+G(d,p) on the B3LYP/6-31+G\* geometries. All the calculations were carried out using the GAUSSIAN 98<sup>20</sup> program installed on the Compaq ES40 computer at the Information Processing Center (Nara University of Education).

## 3. Experimental Results

**3.1.  $X^-(CH_4)_n$ .** As an example, the results of the experimentally measured equilibrium constants for reaction 1 for  $X^- =$

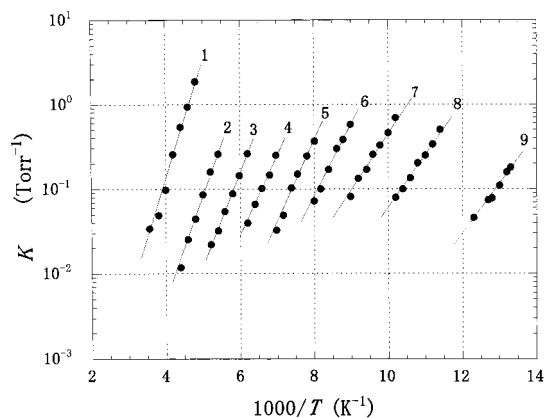


**Figure 1.** van't Hoff plots for the clustering reaction,  $F^-(CH_4)_{n-1} + CH_4 = F^-(CH_4)_n$ .

$F^-$  are displayed in the van't Hoff plots in Figure 1. In Table 1, the enthalpy and entropy changes obtained from the van't Hoff plots for reactions 1 and 2 are summarized.

In Figure 1, irregular decreases of equilibrium constants are observed between  $n = 6$  and  $7$  and also  $n = 8$  and  $9$  for reaction 1 with  $X^- = F^-$ . The slight discontinuous decrease in the bond energies ( $-\Delta H_{n-1,n}^\circ$ ) is also observed with  $n = 6$  and  $8$  in Table 1. The first gap in Figure 1 between  $n = 6$  and  $7$  may be reasonably explained by the formation of the octahedral shell structure with  $n = 6$ . Such a shell completion was also observed for the cluster ion  $F^-(C_2H_4)_n$ .<sup>21</sup> The appearance of the second gap between  $n = 8$  and  $9$  is unique. The sudden decrease in  $-\Delta S_{n-1,n}^\circ$  between  $n = 6$  and  $7$  indicates that the  $n \geq 7$  ligands have more freedom of motion than the  $n \leq 6$  ligands. That is, the rather tight first shell is formed with  $n = 6$ . The somewhat more favorable attachment of two more  $CH_4$  ligands to  $F^-(CH_4)_6$  may be explicable by the accommodation of these two more  $CH_4$  ligands in the two  $C_{3v}$  pockets of the octahedral  $F^-(CH_4)_6$  structure which are opposite to each other. However, the falloff, i.e., the decrease in bond energies in  $F^-(CH_4)_n$  is small in view of other  $F^-(\text{ligand})_n$  clusters.<sup>22</sup> Despite the extremely large nucleophilicity of  $F^-$ , the  $F^- \dots \text{methane}$  interaction is merely of the extent of hydrogen bonds.

**3.2.  $Cl^-(CH_4-mCl_m)_n$ ,  $Cl^-(CH_3Cl)_n$  ( $m = 1$ ).** In Table 1, the bond energies for the cluster ion  $Cl^-(CH_3Cl)_n$  show irregular decrease with  $n = 2, 4$ , and  $6$ . It is surprising that the less nucleophilic reagent  $Cl^-$  than  $F^-$  gives such a decrease. This falloff may be due to the formation of the linear, tetrahedral, and octahedral structures with  $n = 2, 4$ , and  $6$ , respectively. The distinct appearance of the stepwise solvation with even  $n$  values (i.e., 2, 4, and 6) is observed only for  $CH_3Cl$  among  $CH_4-mCl_m$  molecules. This characteristic nature may be due to the interaction of  $CH_3Cl$  with the core ion  $Cl^-$  in such a way that the methyl group of  $CH_3Cl$  attacks the core  $Cl^-$  ion. The values of  $-\Delta S_{n-1,n}^\circ$  in Table 1 decrease with increasing  $n$ ,  $n = 2$  (24 eu)  $\rightarrow n = 4$  (21 eu)  $\rightarrow n = 6$  (18 eu). This suggests that the ligand  $CH_3Cl$  molecules in the cluster ion  $Cl^-(CH_3Cl)_n$  maintain the freedom of motion despite the steric crowd with increase of  $n$  up to  $n = 6$ . The cluster ion seems to prefer the entropy-favored structure rather than the enthalpy-favored one.

**$Cl^-(CH_2Cl_2)_n$  ( $m = 2$ ).** For this cluster, the irregular decrease in the bond energies is observed with  $n = 2$  and  $4$  in Table 1. The  $-\Delta S_{1,2}^\circ$  value (22 eu) is found to be larger than the  $-\Delta S_{3,4}^\circ$  (18 eu). This trend is similar to the case of the  $Cl^-(CH_3Cl)_n$  cluster ion. The cluster ion may be represented as  $Cl^-(CH_2Cl_2)_2(CH_2Cl_2)_{n-4}$ .

**$Cl^-(CHCl_3)_n$  ( $m = 3$ ).** The interactions of halide ions ( $X^-$ ) with neutral molecules (H-R) range widely from hydrogen bond

**TABLE 1: Experimental Thermochemical Data,  $\Delta H_{n-1,n}^\circ$  (kcal/mol) and  $\Delta S_{n-1,n}^\circ$  (cal/mol·K) (standard state, 1 atm) for Gas-Phase Clustering Reactions  $X^-(CH_4)_{n-1} + CH_4 = X^-(CH_4)_n$  and  $Cl^-(CH_4-mCl_m)_n$**

$n$	$F^-(CH_4)_n$	$Cl^-(CH_4)_n$	$Br^-(CH_4)_n$	$I^-(CH_4)_n$	$Cl^-(CH_3Cl)_n$	$Cl^-(CH_2Cl_2)_n$	$Cl^-(CHCl_3)_n$	$Cl^-(C_2H_4)_n$	$-\Delta H_{n-1,n}^\circ$	$-\Delta S_{n-1,n}^\circ$
1	6.7	3.8	3.1	2.6	18	18	18	18	18	18
2	5.9	20	20	11.1	23	20	20	20	19.5	25
3	5.5	3.8	3.1	8.4	15.3 <sup>b</sup>	22 <sup>b</sup>	25	25	19.1 <sup>b</sup>	24.5 <sup>b</sup>
4	5.0	3.8	3.1	7.6	21 <sup>c</sup>	22 <sup>c</sup>	25	25	18.1 <sup>c</sup>	23 <sup>c</sup>
5	4.5	3.8	3.1	6.2	15.8 <sup>c</sup>	22 <sup>c</sup>	25	25	18.1 <sup>d</sup>	22 <sup>d</sup>
6	4.2	3.5	3.5	5.8	13.1	22	25	25	14.7	25
7	3.3	3.5	3.5	4.8	9.7	17	22	22	11.8	22
8	2.9	3.5	3.5	4.8	9.0	18	22	22	9.3	21
9	2.3	3.5	3.5	4.7	7.7	17	22	22	13.4	28
10	1.8	3.5	3.5	4.7	7.7	17	22	22	14.2 <sup>b</sup>	28 <sup>b</sup>

<sup>a</sup> Experimental errors for  $\Delta H^\circ$  and  $\Delta S^\circ$  may be within  $\pm 0.2$  kcal/mol and  $\pm 3$  cal mol<sup>-1</sup> K<sup>-1</sup>, respectively. <sup>b</sup> Ref 26 (Dougherty). <sup>c</sup> Ref 9 (Larson+McMahon). <sup>d</sup> Ref 16 (Grimsrud).

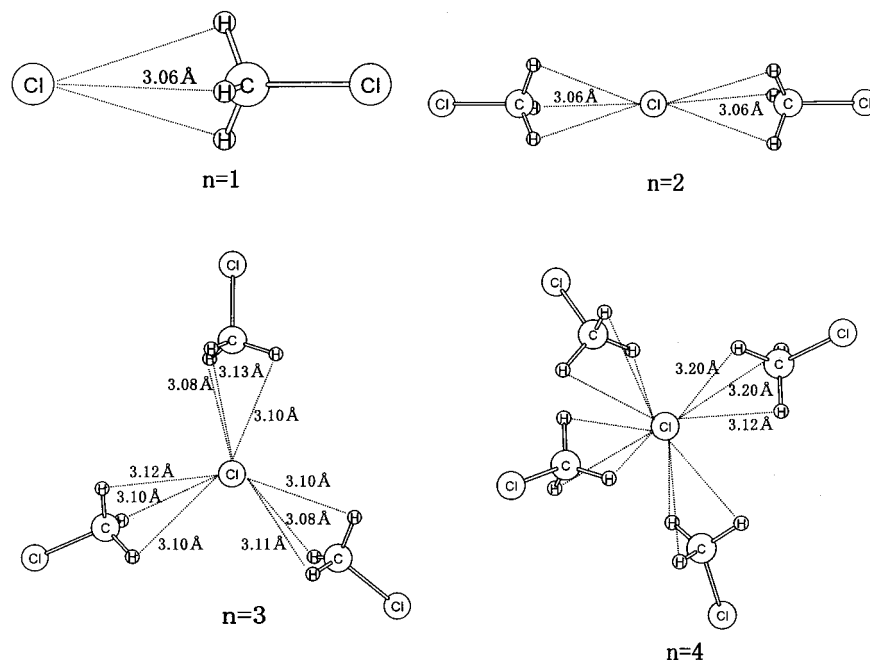


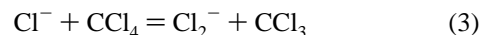
**Figure 2.** Geometries of  $\text{Cl}^-(\text{CH}_2\text{Cl})_n$  ( $n = 1-4$ ).

to electrostatic bond.<sup>22</sup> For instance, the chloride ion forms hydrogen bonds with water, alcohol, and dipolar aprotic solvents (acetone, acetonitrile, etc.) with bond energies ranging from 15 to 20 kcal/mol.<sup>22</sup> In this respect, the bond energy of 19.5 kcal/mol measured here for the cluster ion  $\text{Cl}^-\cdots\text{HCCl}_3$  is a very large one in the  $\text{Cl}^-\cdots\text{H}-\text{R}$  complexes. This must arise from the slight charge transfer in the complex  $\text{Cl}^- \rightarrow \text{HCCl}_3$  since the ion-dipole moment interaction cannot explain this strong bond (permanent dipole moment of  $\text{CHCl}_3$  (1.02 D) is smaller than those of  $\text{CH}_2\text{Cl}_2$  (1.62 D) and  $\text{CH}_3\text{Cl}$  (1.87 D)).<sup>23</sup>

$\text{Cl}^-(\text{CCl}_4)_4$  ( $m = 4$ ). The largest bond energy measured so far for the electrostatic interaction of  $\text{Cl}^-$  ion clusters may be 15.5 kcal/mol for  $\text{Cl}^-\cdots\text{C}_6\text{F}_6$ .<sup>24</sup> The rather weak bond for  $\text{Cl}^-\cdots\text{CO}_2$  (7.6 kcal/mol) arises from the relatively small bond energy of  $\text{Cl}-\text{C}$  covalent bond ( $\sim 78$  kcal/mol).<sup>25</sup> In fact, the reaction of  $\text{F}^-$  with  $\text{CO}_2$  leads to the formation of the fluoroformate ion ( $\text{FCOO}^-$ ) with the bond energy of 32.3 kcal/mol<sup>25</sup> due to the stabilization caused by the formation of the strong  $\text{C}-\text{F}$  bond. The average  $\text{C}-\text{F}$  bond energy is 116 kcal/mol.

In the interaction between  $\text{Cl}^-$  and  $\text{CCl}_4$ , a very small bond energy was expected because of the exchange repulsion between the electron cloud of  $\text{Cl}^-$  and the lone-pair electrons of  $\text{Cl}$  atoms in  $\text{CCl}_4$  molecule. The  $\text{Cl}^-$  ion interacts with rare gas atoms very weakly with bond energies less than a few kilocalories/mole.<sup>26,27</sup> Thus, the bond energy of  $\text{Cl}^-\cdots\text{CCl}_4$  should be definitely much less than 10 kcal/mol. However, surprisingly, the measured bond energy of  $\text{Cl}^-\cdots\text{CCl}_4$  (13.4 kcal/mol) is found to be even larger than that of  $\text{Cl}^-\cdots\text{CH}_3\text{Cl}$  (11.7 kcal/mol) despite the fact that the  $\text{CCl}_4$  has no dipole moment. The unexpectedly large bond energy for  $\text{Cl}^-\cdots\text{CCl}_4$  cannot be explained by the  $\text{S}_{\text{N}}2$  backside coordination structure of  $\text{Cl}^-\cdots\text{Cl}_3\text{CCl}$  because the exchange repulsion prevents the intimate interaction between  $\text{Cl}^-$  and  $\text{CCl}_4$  molecule. As will be described in the latter section, the observed large bond energy was found to be due to the charge dispersal in the complex  $[\text{Cl}\cdots\text{ClCCl}_3]^-$ . The  $\text{Cl}^-$  ion interacts with  $\text{CCl}_4$  linearly along the  $\text{Cl}-\text{C}$  bond axis. The charge dispersal in the complex  $[\text{Cl}\cdots\text{ClCCl}_3]^-$  may arise from the large electron affinities of  $\text{Cl}_2$  (2.3 eV) and  $\text{CCl}_3$  (2.6 eV).<sup>28</sup> Although reactions 3 and 4 are endothermic by 45 and 38 kcal/

mol, respectively, slight charge transfer takes place in the complex  $[\text{Cl}\cdots\text{ClCCl}_3]^-$  resulting in the formation of a rather tight complex



#### 4. Theoretical Results and Discussion

In the previous section, three specific points derived from the present experiment have been discussed (Table 1).

Bond energies of  $\text{F}^-(\text{CH}_4)_n$  decrease rather monotonically as  $n$  grows large despite the significantly large nucleophilicity of  $\text{F}^-$ .

For  $\text{Cl}^-(\text{halomethane})_n$ , there are large decreases in  $n = 2 \rightarrow 3$  bond energies.

For  $\text{Cl}^-(\text{CCl}_4)_n$ , unexpectedly large bond energies have been obtained, which appears to be inconsistent with the prediction that the electronic cloud of  $\text{Cl}^-$  repels lone-pair electrons of  $\text{CCl}_4$ .

In this section, these points are examined with aid of computational results.

In Table 1, the computed bond energies of  $n = 0 \rightarrow 1$  are shown in parentheses. Although they are slightly smaller than those obtained by the present experiment, differences in  $n = 1$  clusters are reasonably reproduced. The small energy,  $\sim 6$  kcal/mol, of  $\text{F}^-(\text{CH}_4)_1$  is confirmed. As expected, symmetric hydrogen-bond geometries of  $\text{F}^-(\text{CH}_4)_n$  ( $n = 1-4$ ) are obtained.  $\text{F}^-\cdots\text{H}$  intermolecular distances are 1.88 Å for  $n = 1$ , 1.92 Å for  $n = 2$  ( $D_{\infty h}$  type), 1.98 Å for  $n = 3$  ( $D_{3h}$  type), and 2.03 Å for  $n = 4$  ( $T_d$  type). The inertness of  $\text{CH}_4$  is exemplified by comparison with the proton-donor character of  $\text{CH}_3-\text{CN}$  (acetonitrile), for example. For  $\text{F}^-(\text{CH}_3\text{CN})_n$ ,  $\Delta H_{0,1}^\circ = -24.5$  kcal/mol, and  $\Delta H_{1,2}^\circ = -17.7$  kcal/mol.<sup>29</sup>  $\text{F}^-\cdots\text{H}$  distances are 1.68 Å for  $n = 1$  and 1.74 Å for  $n = 2$ , where the  $n = 1 \rightarrow 2$  elongation corresponds to the large energy falloff. The smallest  $\text{F}^-\cdots\text{H}$  hydrogen-bond energy involved in  $\text{F}^-(\text{CH}_4)_1$  among  $\text{F}^-$ -centered clusters leads to the slow decrease as  $n$  grows large.

Geometries of  $\text{Cl}^-(\text{CH}_4-m\text{Cl}_m)_n$  ( $m = 1, 2, \text{ and } 4$ ) are

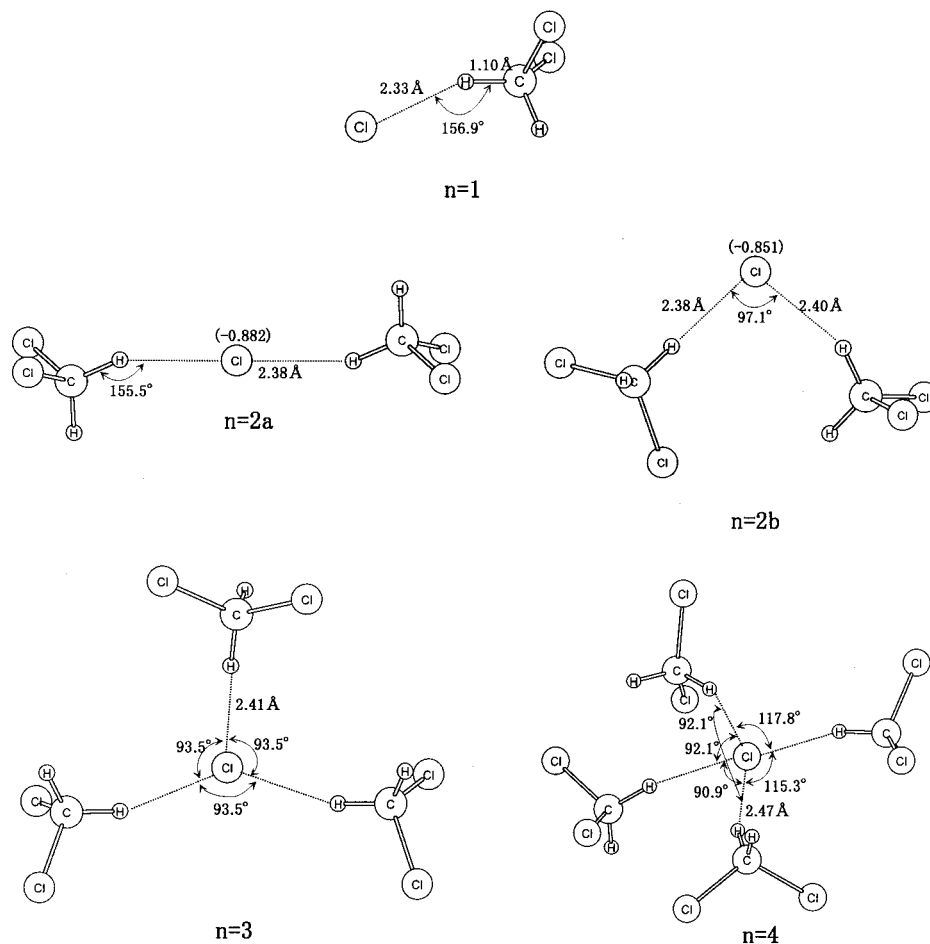


**Figure 3.** Geometries of  $\text{Cl}^-(\text{CH}_2\text{Cl}_2)_n$  ( $n = 1-4$ ). In  $n = 2$ , values in parentheses on the chloride ion denote electronic charges (more negative, more anionic).

examined in detail. Those of  $\text{Cl}^-(\text{CH}_4)_n$  and  $\text{Cl}^-(\text{CHCl}_3)_n$  are obviously hydrogen-bond type, and only a noticeable difference between two clusters are shown;  $\text{CH}\cdots\text{Cl}^-$  hydrogen bond distances are 2.66 Å for  $\text{Cl}^-(\text{CH}_4)_1$  and 2.15 Å for  $\text{Cl}^-(\text{CHCl}_3)_1$ . This large difference corresponds to the remarkable difference in bond energies, 3.8 kcal/mol of  $\text{Cl}^-(\text{CH}_4)_1$  and 19.5 kcal/mol of  $\text{Cl}^-(\text{CHCl}_3)_1$  in Table 1. In Figure 2, geometries of  $\text{Cl}^-(\text{CH}_3\text{Cl})_n$  are shown. The chloride ion is coordinated to the  $C_{3v}$  principal axis in  $\text{Cl}^-(\text{CH}_3\text{Cl})_1$ . This ion-dipole complex geometry is extended to those of larger clusters. The  $\text{Cl}^-\cdots\text{H}$  distance, 3.06 Å, in  $n = 1$  is almost the same as that in  $n = 2$ . The equality indicates that the  $\text{Cl}^-\cdots\text{CH}_3\text{Cl}$  interaction is electrostatic. In  $n = 3$ , the third  $\text{CH}_3\text{Cl}$  molecule works to bend the linear alignment in  $n = 2$ , which corresponds to the appreciable falloff of  $-\Delta H_{n-1,n}^\circ$ , 11.1  $\rightarrow$  8.4 kcal/mol in Table 1. Geometries of  $\text{Cl}^-(\text{CH}_3\text{Cl})_n$  are symmetric ( $D_{\infty h}$  type for  $n = 2$ ,  $D_{3h}$  type for  $n = 3$  and  $T_d$  type for  $n = 4$ ) and are of similar  $\text{Cl}^-\cdots\text{H}$  intermolecular distances owing to the electrostatic attraction.

Figure 3 shows geometries of  $\text{Cl}^-(\text{CH}_2\text{Cl}_2)_n$ . The  $\text{Cl}^-\cdots\text{H}-\text{C}$  angle is  $156.9^\circ$  in  $n = 1$ , which shows that the second hydrogen atom in  $\text{CH}_2\text{Cl}_2$  interacts with  $\text{Cl}^-$  weakly (asymmetric bifurcated form). Despite the slight nonlinearity, the charge-transfer interaction,  $\text{Cl}^- \rightarrow \text{H}-\text{CHCl}_2$ , operates to elongate the  $\text{H}-\text{C}$  bond (1.101 Å relative to 1.087 Å of the free  $\text{CH}_2\text{Cl}_2$ ), which is in contact with  $\text{Cl}^-$ . For  $n = 2$ , linear and orthogonal coordination models were obtained as  $n = 2a$  and  $n = 2b$ , respectively. These isomers have almost the same stability (total energies,  $-2379.714\ 040$  hartree for  $n = 2a$  and  $-2379.714\ 010$

hartree for  $n = 2b$ , 1 hartree = 627.51 kcal/mol). The linear model  $n = 2a$  is obviously due to the electrostatic force. The orthogonal model comes from the charge-transfer force. The difference is understandable by electronic charges ( $-0.882$  of  $n = 2a$  vs  $-0.851$  of  $n = 2b$ ) of  $\text{Cl}^-$ . Since 3s and 3p atomic orbitals on the chloride ion do not hybridize, orthogonal 3p orbital directions are used for the charge donation. Of course, this orthogonal coordination suffers from exchange repulsion between ligand  $\text{CH}_2\text{Cl}_2$  molecules. The equal stability of  $n = 2a$  and  $n = 2b$  indicates the borderline (competition) between electrostatic and charge-transfer forces. For  $n = 2b$ , a slight through-space  $\text{H}\cdots\text{Cl}$  attraction (3.52 Å) is involved. For  $n = 3$ , only the orthogonal model was obtained. An appreciable energy falloff, 13.1 ( $n = 2$ )  $\rightarrow$  9.7 ( $n = 3$ ) kcal/mol, has been observed in  $\text{Cl}^-(\text{CH}_2\text{Cl}_2)_n$  (Table 1). The steric crowd among three  $\text{CH}_2\text{Cl}_2$  ligands results in the decrease of stability for  $\text{Cl}^-(\text{CH}_2\text{Cl}_2)_3$ . For  $n = 4$ , the fourth  $\text{CH}_2\text{Cl}_2$  molecule is linked with  $\text{Cl}^-$  in the less sterically congested direction and undergoes the smallest steric repulsion. In Table 1, a small energy fall off, 9.7 kcal/mol ( $n = 3$ )  $\rightarrow$  9.0 kcal/mol ( $n = 4$ ), has been obtained and is ascribed to the less hindered coordination of  $n = 4$  than that of  $n \leq 3$ . Thus, there is a noticeable contrast between geometries of  $\text{Cl}^-(\text{CH}_3\text{Cl})_n$  (Figure 2) and those of  $\text{Cl}^-(\text{CH}_2\text{Cl}_2)_n$  (Figure 3). They are electrostatic and charge-transfer controlled, respectively.

Figure 4 shows geometries of  $\text{Cl}^-(\text{CCl}_4)_n$  clusters. For  $n = 1$ , two isomers were obtained. The  $n = 1a$  model involves the same backside coordination as that of  $\text{Cl}^-(\text{CH}_3\text{Cl})_1$  (Figure 2).

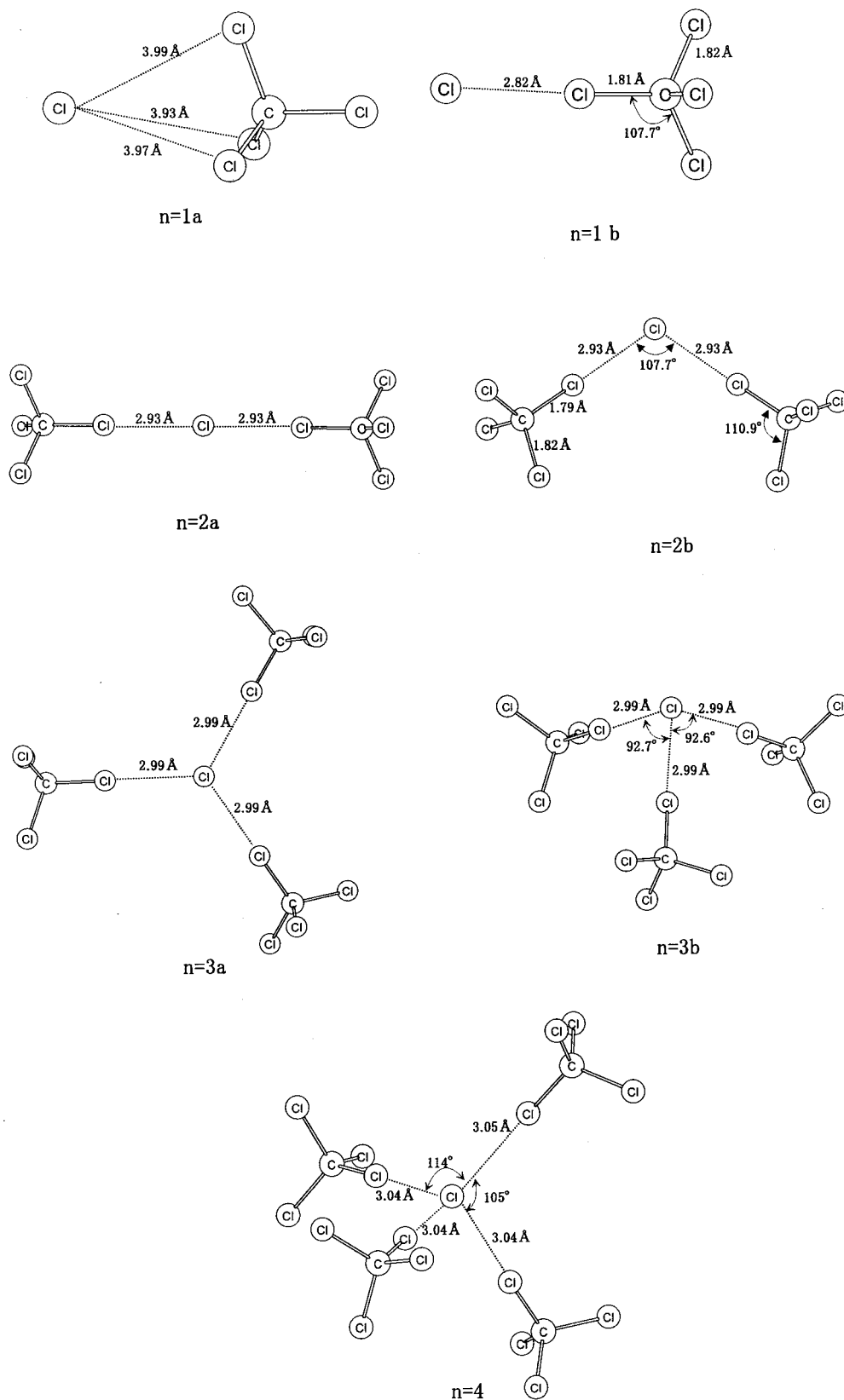
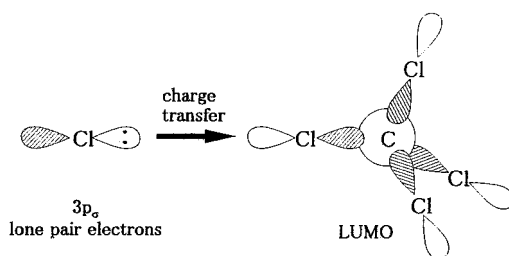


**Figure 4.** Geometries of  $\text{Cl}^-(\text{CCl}_4)_n$  ( $n = 1-4$ ).

Although the  $n = 1a$  geometry is thought to be likely, its  $\text{Cl}^-\dots\text{CCl}_4$  bond energy is only 4.4 kcal/mol, as calculated with QCISD(T)/6-311+G(d,p). This energy is much smaller than that (13.4 kcal/mol) measured in this work. As a more stable model, the isomer  $n = 1b$  was obtained, which has the energy, 10.2 kcal/mol. The  $n = 1b$  geometry is of a surprising linear contact,  $\text{Cl}^-\dots\text{Cl}-\text{CCl}_3$ . Prior to calculations, the geometry could not

be expected, because electronic clouds between two chlorides collide with each other, and the repulsion between  $\text{Cl}^-$  and  $\text{CCl}_4$  would prevail over the attraction. The unexpected  $\text{Cl}^-\dots\text{Cl}-\text{CCl}_3$  "head-on" model needs to be re-considered by means of the charge transfer. In  $\text{CCl}_4$ , four chlorine substituents lower the unoccupied molecular orbitals substantially. Therefore, in terms of energy levels of molecular orbitals,  $\text{CCl}_4$  is a good

electron acceptor (electrophile). The following front-side charge transfer may overcome the exchange repulsion:



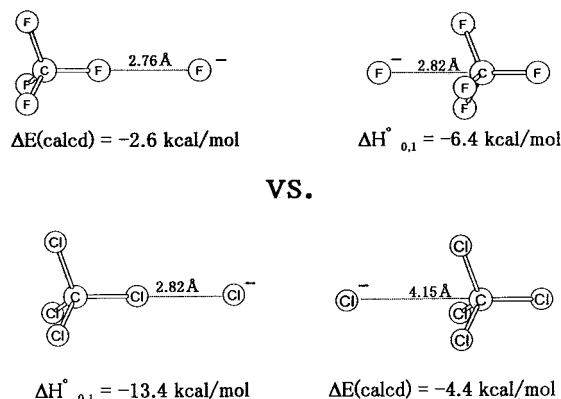
Due to the Cl–C antibonding character of LUMO of  $\text{CCl}_4$ , its charge acceptance leads to the C–Cl elongation (1.70 Å in carbon tetrachloride  $\rightarrow$  1.81 Å in  $\text{Cl}^- \dots \text{Cl}-\text{CCl}_3$  ( $n = 1\text{b}$ )). For  $n = 2$ , there are two geometric isomers. One is an electrostatic controlled linear model,  $n = 2\text{a}$ . The other is a charge-transfer controlled orthogonal one,  $n = 2\text{b}$ . The orthogonality is somewhat incomplete due to the repulsion of spherically large electronic clouds of two  $\text{CCl}_4$  ligands. The  $n = 2\text{b}$  isomer is only 0.25 kcal/mol more stable than the  $n = 2\text{a}$  isomer, which indicates that they are at the borderline in stability. For  $n = 3$ , the electrostatic model  $n = 3\text{a}$  is only 0.50 kcal/mol more stable than the CT one,  $n = 3\text{b}$ . Two  $n = 3$  isomers are again at the borderline. The vague distinction comes from the overlap of diffuse  $3p_\sigma$  orbitals of “soft” chlorine atoms. The vague directionality is in contrast with the relatively clear one of  $\text{Cl}^- \dots \text{H}-\text{CHCl}_2$  hydrogen bonds in  $\text{Cl}^-(\text{CH}_2\text{Cl}_2)_n$  in Figure 3. For  $n = 4$ , intermediate (unclear)  $\text{Cl}^- \dots \text{Cl}^- \dots \text{Cl}$  bond angles were obtained as a mix of the charge-transfer effect and avoidance of steric crowd. Figure 4 has shown the first example of  $\text{Cl}^- \dots \text{Cl}-\text{C}$  linear cluster structures.

In this work, cluster geometries have been calculated by B3LYP/6-31+G\* method. In our previous work,<sup>21</sup>  $\text{X}^-$  (olefin)<sub>n</sub> geometries were obtained both by B3LYP/LANL2DZ(\*,+) and MP4SDQ/6-31+G\*, and the dependence of the two computational methods on the geometries was examined carefully. The B3LYP method includes partially the electron-correlation effect and gave geometric results similar to those by MP4SDQ. Since large clusters [e.g.,  $\text{Cl}^-(\text{CCl}_4)_4$ ] have been examined here, the practical (not so CPU time-consuming) method B3LYP seems to be a suitable choice.

## 5. Concluding Remarks

In this work, gas-phase clustering reactions of halide ions and  $\text{CH}_4-m\text{Cl}_m$  were investigated. The methane molecule is bound very weakly to all halide ions. The  $\text{F}^- \dots \text{H}-\text{CH}_3$  hydrogen bond energy is the smallest one among  $\text{F}^- \dots \text{H}-\text{R}$  combinations. The energy comes mainly from the electrostatic force and leads to symmetric cluster geometries of  $\text{X}^-(\text{CH}_4)_n$ . The symmetric geometries are also found in  $\text{Cl}^-(\text{CH}_3\text{Cl})_n$   $S_N2$  back coordination models. For  $\text{Cl}^-(\text{CH}_4-m\text{Cl}_m)_n$  ( $m = 2-4$ ), charge-transfer interactions prevail over electrostatic interactions. The  $3p$  orbital directions of the chloride ion control orthogonal coordinations of ligand  $\text{CH}_4-m\text{Cl}_m$  molecules. However, orthogonal models suffer from steric hindrance between electronic clouds of  $\text{CH}_4-m\text{Cl}_m$ , particularly at  $n = 3$ . The large energy falloff at  $n = 2 \rightarrow 3$  arises from the steric congestion. Strikingly, the “soft” chloride ion may be coordinated linearly to the Cl–C bond of  $\text{CCl}_4$  with a large bond energy, 13.4 kcal/mol. The anomalous attraction comes from charge-transfer interaction. The anomaly (but generality<sup>32</sup>) is described by the contrast (Scheme 1).

## SCHEME 1: Contrast of $\text{X}^-(\text{CX}_4)_1$ Coordination According to Hardness or Softness of Halogen Atoms and Halide Ions. $\text{F}^-(\text{CF}_4)_1$ Data Are Taken from Ref 31



## References and Notes

- Williams, J. M.; Wang, H. H.; Emge, T. J.; Geiser, U.; Beno, M. A.; Carlson, R. J.; Thorn, K. D.; Schultz, A. J.; Whangbo, M.-H. *Prog. Inorg. Chem.* **1987**, *35*, 51.
- Novoa, J. J.; Whangbo, M.-H.; Williams, J. M. *Chem. Phys. Lett.*, **1991**, *180*, 241.
- Olmstead, W. N.; Brauman, J. I. *J. Am. Chem. Soc.*, **1977**, *99*, 4219.
- Wilbur, J. L.; Brauman, J. I. *J. Am. Chem. Soc.*, **1991**, *113*, 9699.
- Viggiano, A. A.; Paschkewitz, J. S.; Morris, R. A.; Paulson, J. F.; Truhlar, D. G. *J. Am. Chem. Soc.*, **1991**, *113*, 9404.
- Cyr, D. M.; Posey, L. A.; Bishea, G. A.; Han, C.-C.; Johnson, M. A. *J. Am. Chem. Soc.* **1991**, *113*, 9697.
- Graul, S. T.; Bowers, M. T. *J. Am. Chem. Soc.* **1991**, *113*, 9696.
- Peslherbe, G. H.; Wang, H.; Hase, W. L. *J. Chem. Phys.* **1995**, *102*, 5626.
- Li, C.; Ross, P.; Szulejko, J. E.; McMahon, T. B. *J. Am. Chem. Soc.*, **1996**, *118*, 9360.
- Sahlstrom, K. E.; Knighton, W. B.; Grimsrud, E. P. *J. Phys. Chem. A* **1997**, *101*, 5543.
- Mann, D. J.; Hase, W. L. *J. Phys. Chem. A* **1998**, *102*, 6208.
- Raugei, S.; Cardin, G.; Schettino, V. *J. Chem. Phys.* **1999**, *111*, 10887.
- Ayotte, P.; P. Kim, P.; Kelly, J. A.; Nielsen, S. B.; Johnson, M. A. *J. Am. Chem. Soc.*, **1999**, *121*, 6950.
- Li, G.; Hase, W. L. *J. Am. Chem. Soc.*, **1999**, *121*, 7124.
- Larson, J. W.; McMahon, T. B. *J. Am. Chem. Soc.* **1984**, *106*, 517.
- Kebarle, P. In *Techniques for the Study of Ion-Molecule Reactions*; Farrar, J. M., Saunders, W. H., Eds.; Wiley: New York, 1988.
- Hiraoka, K. *J. Chem. Phys.* **1987**, *87*, 4048.
- Becke, A. D. *J. Chem. Phys.* **1993**, *98*, 5648.
- Clark, T.; Chandrasekhar, J.; Spitznagel, G. W.; Schleyer, P. v. R. *J. Comput. Chem.* **1983**, *4*, 294.
- Frisch, M. L.; Trucks, G. W.; Schlegel, H. B.; Scuseria, G. E.; Robb, M. A.; Cheeseman, J. R.; Zakrzewski, V. G.; Montgomery, J. A., Jr.; Stratmann, R. E.; Burant, J. C.; Dapprich, S.; Millam, J. M.; Daniels, A. D.; Kudin, K. N.; Strain, M. C.; Farkas, O.; Tomasi, J.; Barone, V.; Cossi, M.; Cammi, R.; Mennucci, B.; Pomelli, C.; Adamo, C.; Clifford, S.; Ochterski, J.; Petersson, G. A.; Ayala, P. Y.; Cui, Q.; Morokuma, K.; Malick, D. K.; Rabuck, A. D.; Raghavachari, K.; Foresman, J. B.; Cioslowski, J.; Ortiz, J. V.; Baboul, A. G.; Stefanov, B. B.; Liu, G.; Liashenko, A.; Piskorz, P.; Komaromi, I.; Gomperts, R.; Martin, R. L.; Fox, J.; Keith, T.; Al-Laham, M. A.; Peng, C. Y.; Nanayakkara, A.; Gonzalez, C.; Challacombe, M.; Gill, P. M. W.; Johnson, B.; Chen, W.; Wong, M. W.; Andres, J. L.; Gonzalez, J. C.; Head-Gordon, M.; Replogle, E. S.; Pople, J. A. *GAUSSIAN 98*, Revision a.7; Gaussian, Inc.: Pittsburgh, PA, 1998.
- Hiraoka, K.; Katsuragawa, J.; Sugiyama, T.; Kojima, T.; Yamabe, S. *J. Am. Soc. Mass Spectrom.* **2001**, *12*, 144.
- Hiraoka, K.; Yamabe, S.; in: Kuchitsu, K. (Ed.), *Dynamics of Excited Molecules*, Elsevier: Amsterdam, 1994; p.399.
- Nelson, R. D., Jr.; Lide, D. R., Jr.; Maryott, A. A.; *NSRDS-NBS* **1967**, *10*.
- Hiraoka, K.; Mizuse, S.; Yamabe, S. *J. Phys. Chem.* **1987**, *91*, 5294.

- (25) Hiraoka, K.; Mizuse, S.; Yamabe, S. *J. Chem. Phys.* **1987**, *87*, 3647.
- (26) Hiraoka, K.; Sugiyama, T.; Kikkawa, A.; Mizuno, T.; Yamabe, S. *Chem. Phys. Lett.*, to be published.
- (27) Keesee, R. G.; Castleman, A. W. *J. Phys. Chem. Ref. Data* **1986**, *15*, 1011.
- (28) Lias, S. G.; Bartmess, J. E.; Liebman, J. F.; Holmes, J. L.; Levin, R. D.; Mallard, W. G. *Phys. Chem. Ref. Data* *17*, Suppl. No.1, 1989.
- (29) Hiraoka, K.; Mizuse, S.; Yamabe, S. *J. Phys. Chem.* **1988**, *92*, 3943.
- (30) Dougherty, R. C.; Dalton, J.; Roberts, J. D. *Org. Mass Spectrom.* **1974**, *8*, 77.
- (31) Hiraoka, K.; Nasu, M.; Fujimaki, S.; Ignacio, E. W.; Yamabe, S. *Chem. Phys. Lett.* **1995**, *245*, 14.
- (32) For  $\text{Br}^-(\text{CBr}_4)_1$ , the  $\text{Br}^-\cdots\text{Br}-\text{C}$  contact model is 14.2 kcal/mol more favorable than the corresponding  $\text{S}_{\text{N}}2$  model. For  $\text{I}^-(\text{Cl}_4)_1$ , the former model is 21.3 kcal/mol (B3LYP/LANL2DZ(\*,+)) more favorable. The softer X atom prefers the  $\text{X}^-\cdots\text{X}-\text{C}$  contact model.